Journal of Inorganic and General Chemistry
ZAAC
Zeitschrift für anorganische und allgemeine Chemie
www.zaac.wiley-vch.de
RESEARCH ARTICLE
Check for updates
DOI: 10.1002/zaac.202300137

Special Collection

Chromium Metal Nanoparticles, Their Reactivity and Reactions

Andreas Reiß,[a] Maximilian Kai Reimann,[b] Radian Popescu,[c] Dagmar Gerthsen,[c] Rainer Pöttgen,[b] and Claus Feldmann*[a]

Dedicated to Professor Michael Ruck on the occasion of his 60th birthday.

Zerovalent chromium nanoparticles (2.2 ± 0.2 nm in size) are prepared in the liquid phase (THF) by reduction of $CrCl_2$ with lithium naphthalenide ([LiNaph]). The deep black Cr(0) nanoparticle suspensions in THF are colloidally and chemically highly stable. On the other hand, the Cr(0) nanoparticles are highly reactive, e.g., when in contact to O_2, H_2O, or other oxidizing agents. To probe the reactivity of the Cr(0) nanoparticles in the liquid phase near room temperature (50–80 °C), they are reacted with different coordinatively demanding, N–H, S–H or O–H acidic reactants. This includes the amines 2,2′-dipyridylamine (HDPA), 2-(1*H*-imidazol-2-yl)pyridine (HImPy) and carbazole (HCbz), the thiol 2-mercaptopyridine (HMPy), and benzoic acid (HBz) as a carboxylate. As a result, the five novel compounds $[Cr(DPA)_3]$, $[Cr(ImPy)_3]\cdot HImPy$, $[Cr(MPy)_3]\cdot 0.5$ Tol (Tol: toluene), $[Na_2Cr(Cbz)_4(THF)_3]$, and $[Cr_2(Bz)_4(THF)_2]$ are obtained. $[Cr(DPA)_3]$ and $[Cr(ImPy)_3]\cdot HImPy$ show Cr(III) coordinated by nitrogen only; $[Cr(MPy)_3]\cdot 0.5$ Tol shows a coordination of Cr(III) by both N and S atoms. $[Na_2Cr(Cbz)_4(THF)_3]$ and $[Cr_2(Bz)_4(THF)_2]$ contain Cr(II) and exhibit an infinite chain-like structure and pairs of chromium atoms with fourfold binding.

1. Introduction

Chromium is less reactive as a bulk metal. On the one hand, its electrochemical potential (−0.74 eV) is only moderately negative.[1] On the other hand, chromium metal is usually passivated by a thin and dense oxide layer, which is highly relevant to chromium-based steel as it efficiently prevents corrosion.[2] The passivation layer not only hampers reactions with chromium metal but also often leads to oxide impurities. To increase the reactivity of chromium, an option is to use nanoparticles instead of the bulk metal. For nanoparticles the reactivity can be expected to be significantly increased due to the great surface and the high number of insufficiently coordinated surface atoms as well as due to the absence of any metal-oxide passivation layer.[3] Another advantage of small-sized Cr(0) nanoparticles (< 5 nm) relates to their high colloidal stability, which allows reactions in a quasi-homogeneous liquid phase. This guarantees a good mixing of all reactants and a low activation energy for reactions.[4]

Surprisingly, the knowledge on chromium (Cr(0)) nanoparticles is rather limited until now. First of all, so-called activated chromium was reported by *Rieke et al.* but without any particle-specific characterization.[5] Cr(0) particles are yet mainly available with large particle diameters and agglomeration, with chromium-oxide layers for passivation and with elaborate synthesis conditions (e.g. liquid helium droplets).[6] High-quality Cr(0) nanoparticles with small size (< 10 nm) are yet only available via gas-phase methods (e.g., cluster-beam deposition),[7] thermolysis of Fischer carbenes,[8] or in the liquid phase by thermal decomposition of $Cr(CO)_6$ in ionic liquids as shown by *Janiak et al.*.[9] Ligands like alkyls or CO in carbenes or carbonyls as the starting materials, however, can strongly influence the behavior and reactivity of the metal. Finally, publications sometimes claim a synthesis of *"Cr nanoparticles"* but, in fact, refer to chromium oxide nanoparticles.[10]

In the following, we present the synthesis of chromium metal (Cr(0)) nanoparticles via lithium naphthalenide ([LiNaph]) driven reduction of $CrCl_2$ in THF. The reactivity of the Cr(0) nanoparticles was exemplarily probed in the liquid phase near room temperature (50–80 °C) with different coordinatively demanding ligands, including the amines 2,2′-dipyridylamine (HDPA), 2-(1*H*-imidazol-2-yl)pyridine (HImPy), and carbazole

[a] *A. Reiß, Prof. Dr. C. Feldmann*
Institut für Anorganische Chemie
Karlsruhe Institute of Technology (KIT)
Engesserstraße 15, D-76131 Karlsruhe (Germany)
Phone: (+)49-721-60842855
E-mail: claus.feldmann@kit.edu
[b] *Dr. M. K. Reimann, Prof. Dr. R. Pöttgen*
Institut für Anorganische und Analytische Chemie
Universität Münster
Corrensstraße 30, D-48149 Münster (Germany)
[c] *Dr. R. Popescu, Prof. Dr. D. Gerthsen*
Laboratorium für Elektronenmikroskopie
Karlsruhe Institute of Technology (KIT)
Engesserstraße 7, D-76131 Karlsruhe, (Germany)

Supporting information for this article is available on the WWW under https://doi.org/10.1002/zaac.202300137

This article is part of a Special Collection dedicated to Professor Michael Ruck on the occasion of his 60th birthday. Please see our homepage for more articles in the collection.

(HCbz) as well as the thiol 2-mercaptopyridine (HMPy) and benzoic acid (HBz) as a carboxylate. As a result, the new compounds $[Cr(DPA)_3]$ (**1**), $[Cr(ImPy)_3]\cdot HImPy$ (**2**), $[Na_2Cr(Cbz)_4(THF)_3]$ (**3**), $[Cr(MPy)_3]\cdot 0.5$ Tol (**4**, Tol: toluene), and $[Cr_2(Bz)_4(THF)_2]$ (**5**) were obtained and characterized by single-crystal structure analysis and FT-IR spectroscopy. Exemplarily, specific properties such as color and magnetism of **1** and **2** were examined in detail.

2. Results and discussion

2.1 Chromium metal nanoparticles

In principle, the synthesis of Cr(0) nanoparticles follows our recently developed strategy for obtaining base-metal nanoparticles.[11] Specifically, $CrCl_2$ was reduced by lithium naphthalenide ([LiNaph]) in tetrahydrofurane (THF) (Figure 1a). A specific difficulty of the synthesis relates to the very low solubility of $CrCl_2$ or $CrCl_3$ in ethers. In contrast to other base-metal nanoparticles (e.g. rare-earth metals),[11] a reduction of the metal halide by injection of [LiNaph] in an homogeneous solution was not possible. To our surprise, we realized that the formation of Cr(0) nanoparticles can be performed as a one-pot reaction nevertheless by simultaneous addition of lithium, naphthalene, and $CrCl_2$ in THF. Whereas [LiNaph] was instantaneously formed and dissolved, $CrCl_2$ remained as an insoluble solid. Due to the very slow dissolution of $CrCl_2$ (over several hours) but the very fast reduction after dissolution, Cr(0) nanoparticles with small and uniform size were obtained nevertheless. After 12 hours with intense stirring, the dissolution of $CrCl_2$ and the reduction were completed, resulting in a deep-black suspension of Cr(0) nanoparticles (Figure 1b).

For purification, the as-prepared Cr(0) nanoparticles were centrifugated/redispersed in/from a 1:1 mixture of toluene and THF to remove remaining starting materials, naphthalene and LiCl. Finally, the Cr(0) nanoparticles were redispersed in THF or toluene to obtain colloidally stable suspensions. Alternatively, the nanoparticles can be dried at room temperature in vacuum to obtain powder samples with a yield of about 80% (losses mainly due to incomplete centrifugation). Suspensions and powder samples are chemically stable under inert conditions (argon, nitrogen), whereas they show violent reactions when in contact with air or water. In regard of a well-reproducible one-pot synthesis, the high yield, and the high stability under inert conditions, the Cr(0) nanoparticles can be considered as a suitable starting material, which is much more reactive than bulk chromium.

Particle size and particle size distribution of the as-prepared Cr(0) nanoparticles were examined by transmission electron microscopy (TEM). Accordingly, TEM images show spherical particles with a uniform size of 2–3 nm and a low degree of agglomeration (Figure 2a). A statistical evaluation of >150 nanoparticles on TEM images reveals a mean diameter of 2.2 ± 0.2 nm (Figure 2b). High-resolution (HR)TEM images confirm the size of the nanoparticles and show the crystallinity of the as-prepared Cr(0) with lattice fringes extending through the whole particle (Figures 2c). The average fringe distance of 2.0 ± 0.1 Å is in agreement with the (011) lattice-plane distance of cubic bulk α-Cr ($d_{011}=2.04$ Å).[12] This finding is also confirmed by Fourier-transform (FT) analysis, which is in accordance with the calculated diffraction pattern of body-centered cubic chromium metal in the [001] zone axis (space group $Im\bar{3}m$, $a=2.8849$ Å, Figure 2d).[12] The intensity of the Bragg reflections is of course low due to the small size and limited scattering power of the Cr(0) nanoparticles.

Figure 1. Scheme illustrating the liquid-phase synthesis of Cr(0) nanoparticles and exemplary follow-up reactions with quasi-homogeneous conditions: a) starting materials prior to mixing and formation of [LiNaph], b) as-prepared suspension of Cr(0) nanoparticles in THF, c) reaction of the Cr(0) nanoparticles near room temperature with HDPA, HImPy, HMPy, HCbz, and HBz to obtain single crystals (up to 0.5 mm in size) of **1**–**5**.

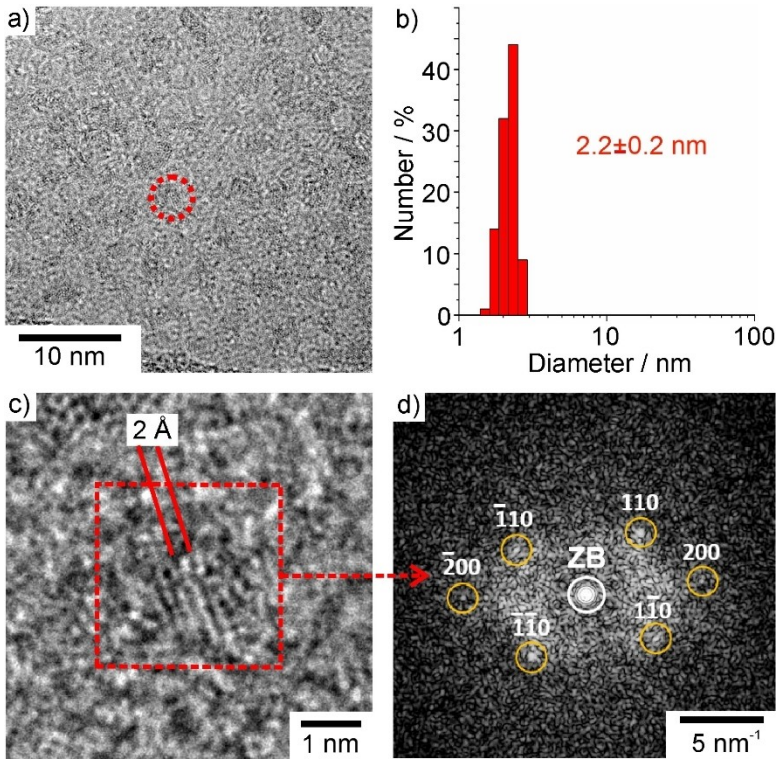

Figure 2. Size and size distribution of the as-prepared Cr(0) nanoparticles with a) TEM overview image (single Cr(0) nanoparticle exemplarily marked by red dots), b) size distribution based on a statistical evaluation of >150 nanoparticles on TEM images, c) HRTEM image of Cr(0) nanoparticle with lattice fringes, d) FT analysis of a single nanoparticle with reflections compared to calculated diffraction pattern of bulk body-centered cubic α-Cr (yellow circles) in the [001]-zone axis (zero-order beam marked by white circle).

In regard of a use of the as-prepared Cr(0) nanoparticles for follow-up reactions, their surface functionalization is important. Generally, nanoparticles made via liquid-phase syntheses as a matter of course have at least the solvent adhered on the surface (designated as "quasi-naked" nanoparticle).[13] To this concern, Fourier-transformed infrared (FT-IR) spectroscopy only shows the vibrations of THF (Figure 3a), whereas naphthalene and toluene are not observed. Furthermore, elemental analysis (EA) shows C/H contents of 0.8 and 2.0 mol%, which reflects the C/H ratio in THF. The instantaneous reaction of Cr(0) nanoparticle powders when in contact to air already indicates their high reactivity and the absence of strongly coordinating ligands or oxide layers passivating the surface (Figure 3b). The absence of any strong binding and/or high-molecular-weight surface functionalization offers the option for reactions with other reactants and without the ingredients of the initial nanoparticle synthesis dominating or even deteriorating the follow-up reactions and products.

2.2 Follow-up reactions

Reactions with the as-prepared Cr(0) nanoparticles were performed with quasi-homogenous conditions in toluene (Tol) near room temperature ($\leq 100\,^{\circ}C$). To probe the reactivity of the metal nanoparticles, they were reacted with the amines 2,2′-dipyridylamine (HDPA), 2-(1*H*-imidazol-2-yl)pyridine (HImPy), carbazole (HCbz) as well as the thiol 2-mercaptopyridine (HMPy) and the carboxylate benzoic acid (HBz). On the one hand, these N–H, S–H or O–H acidic reactants have certain size and are coordinatively demanding. On the other hand, they offer different options for deprotonation and coordination via different heteroatoms. The compounds $[Cr(DPA)_3]$ (**1**) and $[Cr(ImPy)_3]\cdot HImPy$ (**2**) were characterized in detail.

To perform follow-up reactions with HDPA and HImPy, the as-prepared Cr(0) nanoparticles were washed (i.e. twice centrifuged/redispersed from/in a 1:1 mixture of THF and toluene) to remove all dissolved salts and excess starting materials. Then, the Cr(0) nanoparticles were centrifuged and dried in vacuum to remove the liquid phase. Drying was performed at room temperature to avoid any temperature-induced agglomeration of the nanoparticles and/or reaction with surface-adhered THF. Thereafter, the N–H acidic reactants HDPA or HImPy were added to the dried Cr(0) nanoparticles. Moreover, few drops of Tol were added. After heating to 80 °C for 7 days, deep-red and orange crystals of pure $[Cr(DPA)_3]$ (**1**) and $[Cr(ImPy)_3]\cdot HImPy$ (**2**) were formed according to the following reactions (Figure 1c):

$$2\ Cr + 6\ HDPA \leftrightarrow 2\ [Cr(DPA)_3] + 3\ H_2$$

$$2\ Cr + 8\ HImPy \leftrightarrow 2\ [Cr(ImPy)_3] \cdot HImPy + 3\ H_2$$

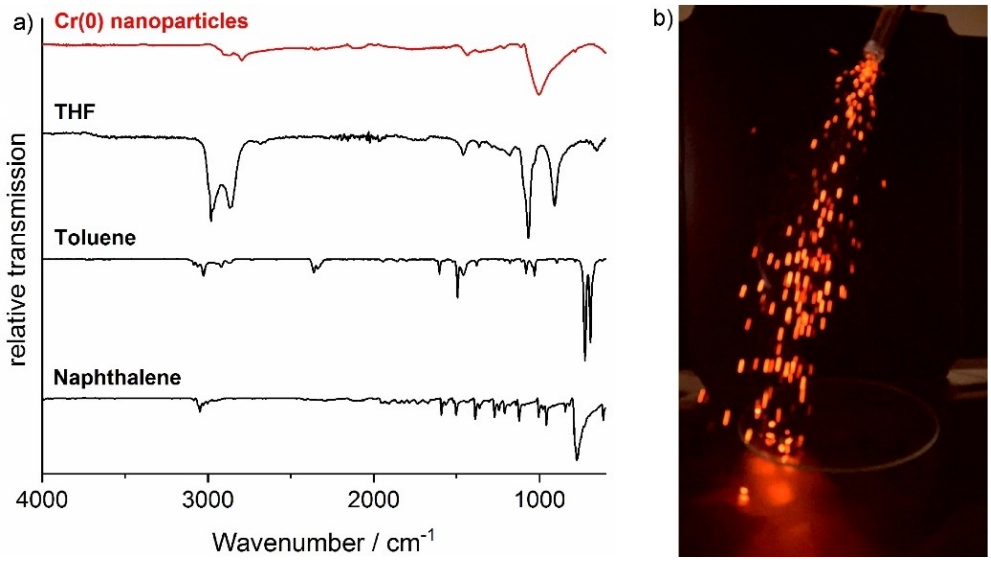

Figure 3. Surface conditioning and reactivity of the as-prepared Cr(0) nanoparticles: a) FT-IR spectrum with THF, toluene, and naphthalene as references; b) Photo showing the reaction of powder samples (20 mg) in air.

1 and **2** were obtained with a yields of about 50 and 90% based on the amount of obtained crystals, which is limited by the fact that the title compounds partially remain dissolved in toluene. Finally, it needs to be noticed that all reactions need to be performed with inert conditions (i.e., dried solvent, Ar atmosphere, Schlenk tubes) due to the sensitivity of the Cr(0) nanoparticles, whereas the resulting Cr(III) compounds were stable in air for several hours.

According to single-crystal structure analysis (*SI: Table S1; Figures S1, S2*), **1** and **2** crystallize in the orthorhombic space group *Pbca* and the triclinic space group $P\bar{1}$, respectively. Both compounds exhibit a distorted octahedral coordination of the Cr(III) center with nitrogen of three η^2-coordinating ligands (Figure 4). Thus, the N–H acidic reactants were deprotonated to $[DPA]^-$ and $[ImPy]^-$. Moreover, an additional non-coordinating HImPy molecule is present in **2**. The Cr–N distances range from 204.0(2)–207.1(2) pm in **1** to 199.6(3)–210.2(2) pm in **2**. These distances are in good agreement with, for instance, Cr(III)N (207 pm)[14] or $[Cr(III)(NH_3)_6]^{3+}$ (224 pm).[15] The N–Cr–N angles range from 64.8(1)–178.0(1)° in **1** and 79.7(1)–175.1(1)° in **2**, indicating the distorted octahedral arrangement. The octahedral coordination with three sterically demanding ligands also explains the good stability and the slow hydrolysis of both title compounds.

Beside single-crystal structure analysis, composition and purity of **1** and **2** were confirmed by Fourier-transform infrared (FT-IR) spectroscopy and elemental analysis (EA). To this concern, FT-IR spectra of $[Cr(DPA)_3]$ and $[Cr(ImPy)_3]\cdot HImPy$ show

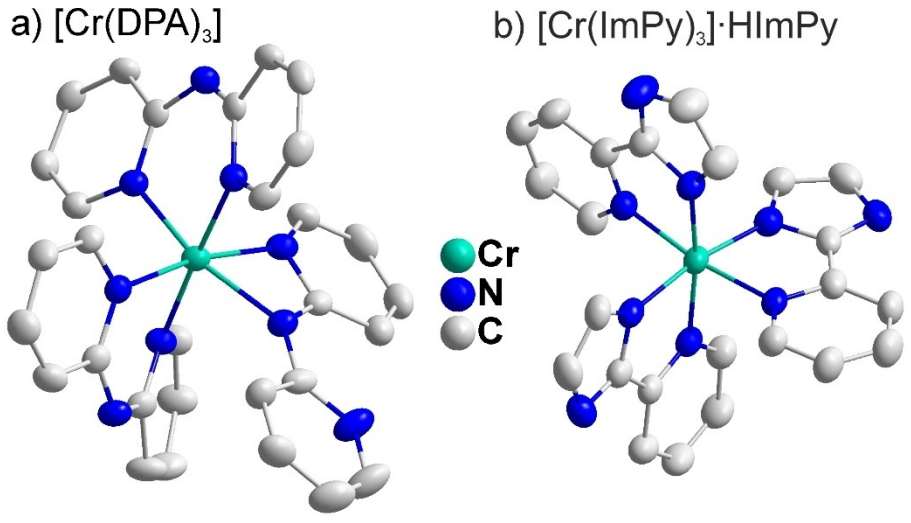

Figure 4. Structure of the nitrogen-coordinated title compounds **1** (a) and **2** (b).

Journal of Inorganic and General Chemistry
ZAAC
Zeitschrift für anorganische und allgemeine Chemie

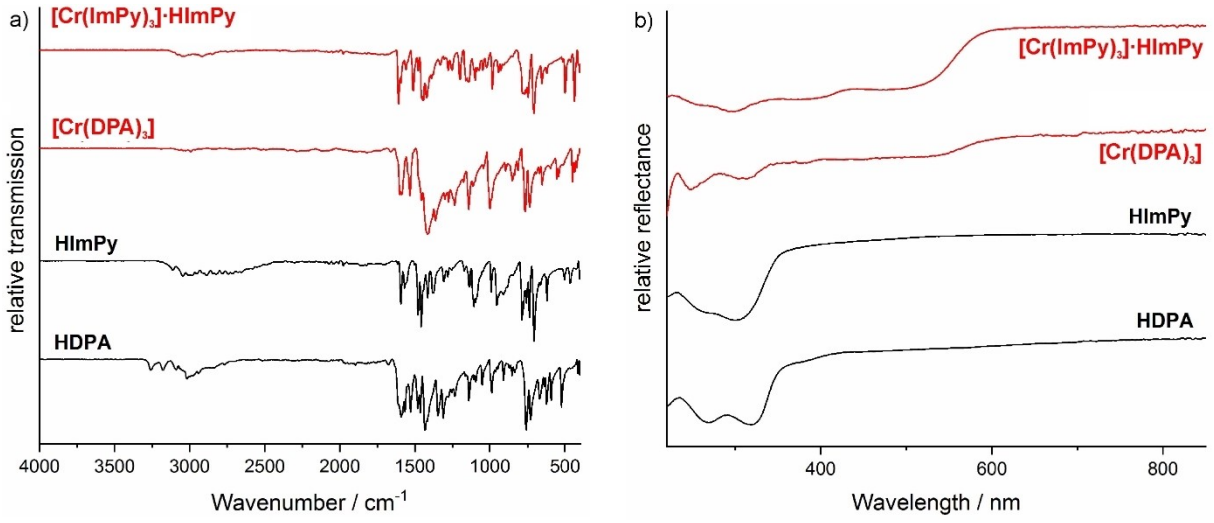

Figure 5. FT-IR (a) and UV-Vis (b) spectra of the title compounds **1** and **2** (with the free ligands HImPy and HDPA as references).

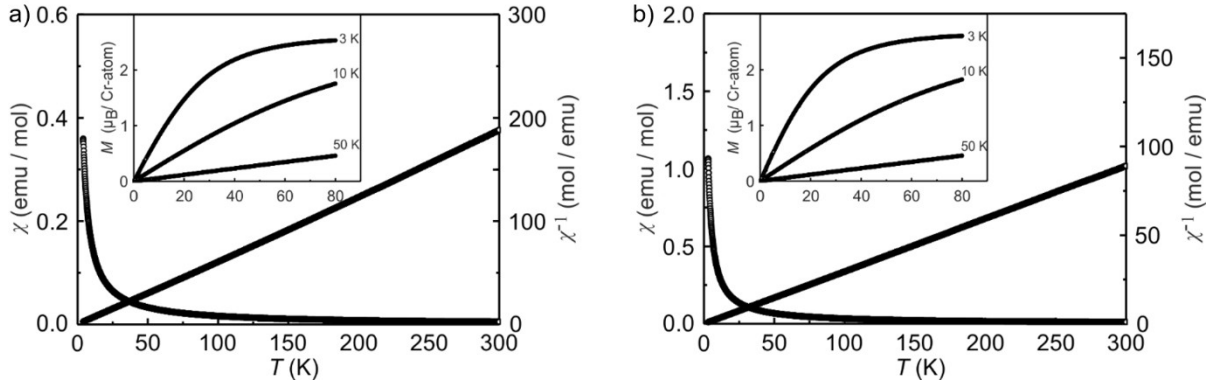

Figure 6. Magnetic properties of a) $[Cr(DPA)_3]$ and b) $[Cr(ImPy)_3]\cdot HImPy$ with temperature dependence of the magnetic susceptibility and its inverse (χ and χ^{-1} data) recorded with an external field of 10 kOe (insets show the magnetic magnetization isotherms at 3, 10, 50 K).

the expected characteristic vibrations of the respective ligands, which are shown as a reference in addition (Figure 5a). Most interestingly, the N–H vibrations at 3250–2800 cm^{-1} vanish completely for $[Cr(DPA)_3]$ and are significantly reduced in intensity for $[Cr(ImPy)_3]\cdot HImPy$, which confirms the deprotonation of the ligand. EA shows 21.0 wt% N, 60.7 wt% C, 4.1 wt% H for **1** and 25.9 wt% N, 60.7 wt% C, 4.0 wt% H for **2**, which is in accordance with the calculated values (**1**: 22.4 wt% N, 64.1 wt% C, 4.3 wt% H; **2**: 26.7 wt% N, 61.0 wt% C, 4.0 wt% H). In both cases, the remaining difference can be attributed to chromium. Furthermore, the color of **1** and **2** was quantified by optical spectroscopy (UV-Vis) (Figure 5b). Accordingly, a strong absorption below 600 nm is observed and reflects the deep-red or orange color of **1** and **2**. Shape and intensity of the absorption are in accordance with a $d \rightarrow d$ transition.

Crystal structure, bond distances and electroneutrality already suggest an oxidation state of +III for chromium for the title compounds **1** and **2**. To validate the oxidation state, the temperature dependence of the magnetic susceptibility of $[Cr(DPA)_3]$ and $[Cr(ImPy)_3]\cdot HImPy$ (χ and χ^{-1} data) were exemplarily examined (Figure 6). Both compounds show Curie-Weiss behavior within the entire temperature range. The experimental data derived from the fits according to the Curie-Weiss law are summarized in Table 1. The experimental magnetic moments of 3.68(1) μ_B/Cr atom for **1** and 3.66(1) μ_B/Cr atom for **2** are close to the free ion value of 3.87 μ_B for Cr^{3+} ($S = 3/2$) according to $2[S(S+1)]^{1/2}$,[16] indicating stable trivalent

Table 1. Magnetic properties of $[Cr(DPA)_3]$ and $[Cr(ImPy)_3]\cdot HImPy$, with μ_{eff}, effective magnetic moment, μ_{calc}, calculated magnetic moment, θ_p, paramagnetic Curie temperature, μ_{sat} saturation moment and calculated saturation magnetization according to $g_J \times J$.

Compound	μ_{eff}/μ_B	$\mu_{eff,theo}/\mu_B$	θ_p/K	μ_{sat}/μ_B	$g_J \times J/\mu_B$
$[Cr(DPA)_3]$	3.68(1)	3.87	−0.78(3)	2.53(1)	3
$[Cr(ImPy)_3]\cdot HImPy$	3.66(1)	3.87	0.94(3)	2.61(1)	3

chromium. The Weiss constants derived from the fits are negligible, indicating almost Curie-like behavior. The inserts show the magnetization isotherms at 3, 10 and 50 K (Figure 6). Both 50 K isotherms show a strictly linear increase with low absolute values, as expected for a paramagnetic compound. Slightly higher values along with slight curvature are observed at 10 K. Finally, a tendency towards Brillouin type behavior was observed for the 3 K isotherms. They exhibit much stronger curvature and tend towards saturation. The magnetic moments at 3 K and 80 kOe of 2.53(1) μ_B/Cr atom for **1** and 2.61(1) μ_B/Cr atom for **2** almost reach the theoretical saturation magnetization of Cr^{3+} ($g_J = 2$ and $J = 3/2$) of 3 μ_B/Cr atom according to $\mu_{sm(calc)} = g_J \times J$.[16]

In addition to the reactions with HDPA or HImPy, the Cr(0) nanoparticles were reacted with carbazole (HCbz), 2-mercaptopyridine (HMPy), and benzoic acid (HBz), using similar conditions as for the compounds **1** and **2**. After 7 days of heating at 50–80 °C, the compounds $[Cr(MPy)_3]$ (**3**), $[Na_2Cr(Cbz)_4(THF)_3]$ (**4**), and $[Cr_2(Bz)_4(THF)_2]$ (**5**) were obtained as red, deep green and yellow-brown crystals (Figure 1c). Composition and structure of these compounds were characterized by single-crystal structure analysis and FT-IR spectroscopy (*SI: Table S1, Figures S3–S8*). Similar to $[Cr(DPA)_3]$, the N–H vibrations (3250–2800 cm^{-1}) of HCbz and HMPy as well as the COO–H vibrations of HBz (3200–2600 cm^{-1}) vanish completely for the compounds **3**–**5**, respectively, which similar to **2** confirms the deprotonation of the ligands. The formation of **3**–**5** can be again rationalized based on a liquid-phase oxidation of chromium and a reduction of the respective N–H, S–H or O–H acidic reactants with the formation of hydrogen:

$$2\ Cr + 4\ HCbz + 2\ NaCl + 3\ THF \leftrightarrow [Na_2Cr(Cbz)_4(THF)_3] + CrCl_2 + 2\ H_2$$

$$2\ Cr + 6\ HMPy + 0.5\ Tol \leftrightarrow 2\ [Cr(MPy)_3] \cdot 0.5\ Tol + 3\ H_2$$

$$2\ Cr + 4\ HBz + 2\ THF \leftrightarrow [Cr_2(Bz)_4(THF)_2] + 2\ H_2$$

$[Na_2Cr(Cbz)_4(THF)_3]$ (**3**) crystallizes in the monoclinic space group $P2_1/c$ (*SI: Table S1, Figure S3*). Surprisingly, each Cr atom is coordinated by four of the voluminous Cbz ligands in a square-planar arrangement (Figure 7a). Such coordination was observed for Cr(II) with other voluminous ligands (e.g., bis(trimethylsilyl)amide, 1,2-bis(diisopropylphosphino)ethane, 3,6-bis(trimethylsilyl)benzene-1,2-dithiolate)[17] but is here first observed with the Cbz ligand. Furthermore, sodium is present in the crystal structure of **3** and interlinks the $Cr(Cbz)_4$ units to infinite zigzag chains. It needs to be noted that **3** can be obtained only if [NaNaph] was applied for the formation of the Cr(0) nanoparticles instead of [LiNaph]. Thus, Na^+ in **3** originates from the reducing agent to prepare the Cr(0) nanoparticles. Na^+ shows non-covalent interactions with Cbz, comprising η^6-interaction with one Cbz ligand and η^2-interaction with two additional Cbz ligands (Figure 7a). Furthermore, one or two THF molecules are coordinated to the two crystallographically different Na^+ cations. Based on four negatively charged Cbz ligands and two Na^+ cations per formula unit, finally, chromium can be concluded to exhibit an oxidation state of +II. The Cr–N distances in **3** are 204.6(1)–207.2(2) pm. These distances match well with few already known carbazole-containing Cr(II) complexes (Table 2). Here, it needs to be noticed that known Cr(II) complexes contain either sterically demanding carbazole ligands or carbazole derivatives as pincer-type ligands.[18] The Na–O distances range from 227.0(2) to 232.2(2) pm; the Na–C distances range from 280.5(2)–308.2(2) pm. Finally, the N–Cr–N angles are 88.2(1)–91.7(1)°, again indicating a distorted square-planar arrangement.

According to single-crystal structure analysis, $[Cr(MPy)_3] \cdot 0.5$ Tol (**4**) crystallizes in the triclinic space group $P\bar{1}$ (*SI: Table S1, Figure S4*). Herein, a Cr(III) center is η^2-coordinated by three MPy ligands via both the N and the S heteroatom to result in a distorted octahedron (Figure 7b). In addition, Tol is located as an isolated, non-coordinating molecule between the $[Cr(MPy)_3]$ building units. Although **4** is firstly observed as a compound, octahedral coordination of Cr(III) by three MPy ligands was already described in the literature.[18] The Cr–N distances in **4** range from 203.2(2) to 205.4(2) pm and the Cr–S distances from 239.4(1) to 240.6(1) pm, which is in good agreement with literature data (Cr–N: 203.7(4)–204.2(4) pm, Cr–S: 239.68(12)–240.77(13) pm).[19] N–Cr–N and S–Cr–S angles of 93.7(1)–99.2(1)° and 97.7(1)–98.5(1)° point to the distorted octahedral arrangement.

$[Cr_2(Bz)_4(THF)_2]$ (**5**) crystallizes in the monoclinic space group $P2_1/n$ (*SI: Table S1, Figure S5*). Herein, pairs of Cr(II) atoms with fourfold metal-metal binding are observed (Figure 7c). The Cr≡Cr couple is bridged by four μ_2-binding Bz ligands. Finally, the coordination is completed by terminal binding of THF to each of the Cr(II) atoms. Such Cr≡Cr couples with paddlewheel-type ligand coordination are well-known in the literature, comprising differently substituted acetate- and benzoate-based ligands.[20] The composition of **4** was already suggested but only examined by infrared spectroscopy.[21] The crystal structure of **4** is reported here for the first time. The Cr≡Cr distance in **5** is 232.6(1) pm, which matches with other compounds containing Cr(II) pairs with fourfold binding (231.9(2)–236.6(1) pm).[20b] The Cr–O distances range from of 200.3(1)–201.8(1) pm for the Bz ligands and 227.1(1) pm for the THF ligand.

In sum, the follow-up reactions and the formation and crystallization of the compounds **1**–**5**, first of all, indicate the suitability of Cr(0) nanoparticles as a starting material in the liquid phase at moderate temperatures. Although THF and Na^+ are present in **3** and **5**, which originate from the synthesis of the Cr(0) nanoparticles (i.e. THF as solvent, Na^+ from [NaNaph]), the ingredients of the original Cr(0) nanoparticle synthesis

Table 2. Cr–N distances (pm) of **3** in comparison to literature-known compounds.

Compound	Cr–N distance
3	204.6(2)–207.1(2)
$[(1,8\text{-}Ph_2\text{-}3,6\text{-}Me_2C_{12}H_4N)_2Cr]$[18a]	207 (calculated value)
$[^{iPr}(PNP)Cr(\mu\text{-}H)]_2$[18b]	205.5(1)

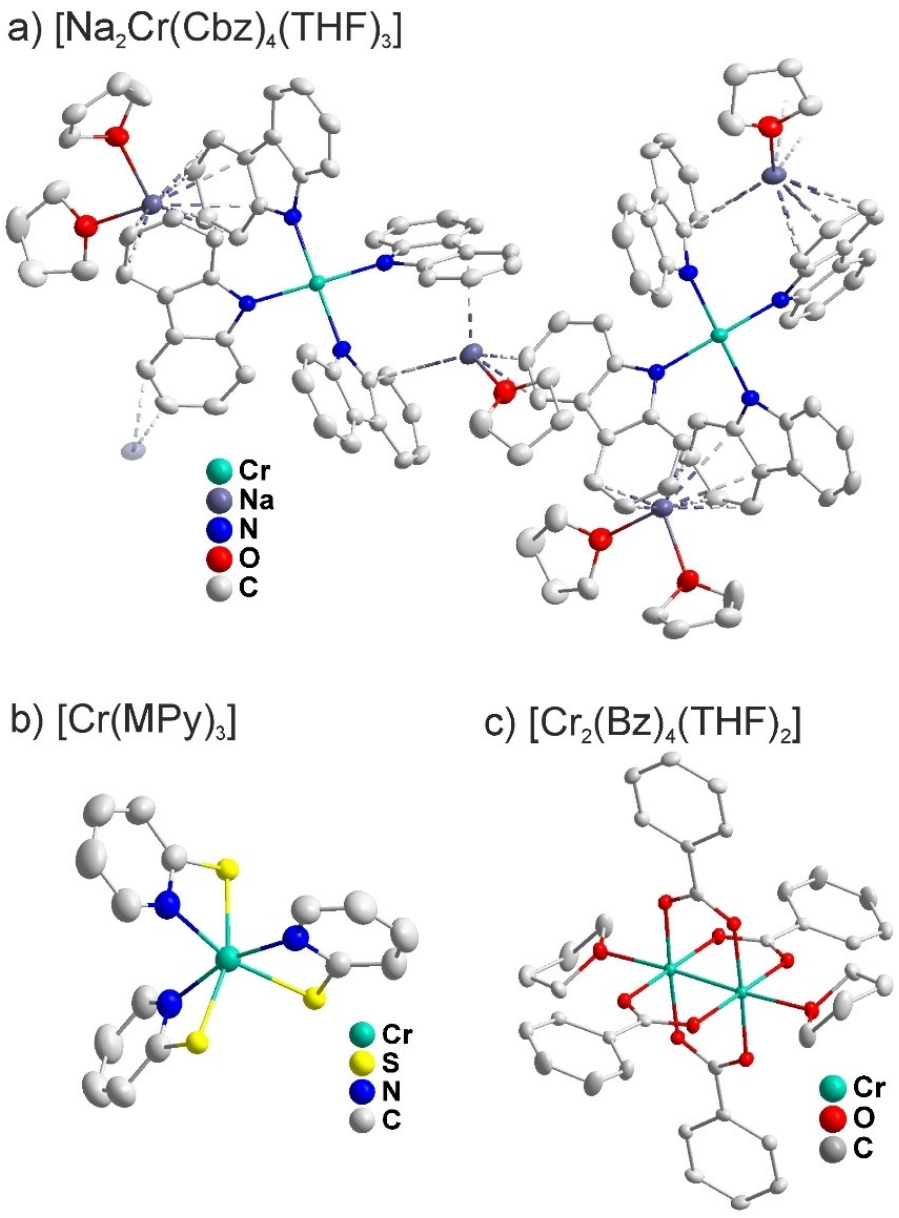

Figure 7. Structure of the title compounds **3** (a), **4** (b) and **5** (c).

neither occur in all compounds nor do they dominate the reactions and products.

3. Conclusions

Zerovalent chromium nanoparticles are prepared for the first time in the liquid phase (THF) by reduction of $CrCl_2$ with lithium naphthalenide ([LiNaph]). The as-prepared suspensions are colloidally highly stable and contain uniform, small-sized and crystalline Cr(0) nanoparticles with a diameter of 2.2 ± 0.2 nm. Due to the small size, the great number of surface atoms and the absence of oxide passivation layers, the Cr(0) nanoparticles are highly reactive even at room temperature as indicated by the violent reaction with O_2 (air). To probe the reactivity of the Cr(0) nanoparticles in the liquid phase (Tol) near room temperature (50-80 °C), they were exemplarily reacted with coordinatively demanding N–H, S–H or O–H acidic reactants, including 2,2′-dipyridylamine (HDPA), 2-(1*H*-imidazol-2-yl)pyridine (HImPy) and carbazole (HCbz) as amines, the thiol 2-mercaptopyridine (HMPy), and the carboxylate benzoic acid (HBz). These reactions lead to $[Cr(DPA)_3]$, $[Cr(ImPy)_3]\cdot HImPy$, $[Cr(MPy)_3]\cdot 0.5$ Tol, $[Na_2Cr(Cbz)_4(THF)_3]$, and $[Cr_2(Bz)_4(THF)_2]$ as new compounds. In regard of the use of Cr(0) nanoparticles as a starting material, it needs to be noticed that the ingredients of the original Cr(0) nanoparticle synthesis neither occur in all compounds nor do they dominate the reaction and product. In regard of the obtained products, different coordinative scenarios are obtained with

different multidentate ligands and different heteroatoms. Cr(III) as well as Cr(II) are realized as metal centers as well as fourfold binding of chromium pairs. Altogether, reactivity and reactions of the Cr(0) nanoparticles offer the option to prepare many more new compounds with quasi-homogeneous conditions near room temperature.

Experimental

General aspects. All sample handling and reactions were performed under argon atmosphere using standard Schlenk techniques and gloveboxes (MBraun Unilab, $O_2/H_2O < 1$ ppm). Prior to use, all glassware was evacuated ($p \leq 10^{-3}$ mbar), heated, and flushed with argon three times to remove all moisture.

Chemicals. Tetrahydrofurane (THF, Seulberger, 99%) and toluene (Seulberger, 99%) were refluxed over sodium with benzophenone and distilled prior to use. Lithium metal (Alfa Aesar, 99%) as well as sodium metal (Riedel-de-Haën, 99%) were freshly cut under argon atmosphere prior to use. 2,2′-Dipyridylamine (HDPA, Sigma-Aldrich, 98%), 2-(1*H*-imidazol-2-yl)pyridine (HImPy, Sigma-Aldrich, 97%), carbazole (HCbz, Sigma-Aldrich, >95%), 2-mercaptopyridine (HMPy, Sigma-Aldrich, 99%), benzoic acid (HBz, Sigma-Aldrich, 99%), chromium(II) chloride (Alfa Aesar, 99.9%) and naphthalene (Alfa Aesar, ≥99%) were used as purchased.

Cr(0) nanoparticles. 9.3 mg of lithium or 30.8 mg of sodium (1.34 mmol) and 180 mg of naphthalene (1.40 mmol) were dissolved in 15 mL of THF. 82.3 mg of $CrCl_2$ (0.67 mmol) were added and stirred for 12 h. The resulting deep black suspension was centrifuged to separate the Cr(0) nanoparticles. To remove excess starting materials, naphthalene and LiCl, the nanoparticles were redispersed/centrifuged in/from 15 mL of a 1:1 mixture of toluene and THF. Finally, the Cr(0) nanoparticles were redispersed in THF or toluene or dried in vacuum (20 min) to obtain powder samples with a yield of about 80%. Certain loss of nanoparticles can be ascribed to the purification process and predominately nanoparticles sticking on the wall of the centrifuge tubes.

$[Cr(DPA)_3]$ (1). 37.5 mg of HDPA (0.22 mmol) and 0.15 mL of toluene were added to 22.7 mg of the Cr(0) nanoparticles (0.44 mmol) in an argon-filled Schlenk tube (20 mL). This Schlenk tube was heated to 80 °C for 7 days. After cooling to room temperature, deep red crystals of **1** were obtained with a yield of about 50%.

$[Cr(ImPy)_3]\cdot HImPy$ (2). 63.4 mg of HImPy (0.44 mmol) and 0.15 mL of toluene were added to 22.7 mg of the Cr(0) nanoparticles (0.44 mmol) in an argon-filled Schlenk tube (20 mL). This Schlenk tube was heated to 80 °C for 7 days. After cooling to room temperature, orange crystals of **2** were obtained with a yield of about 90%.

$[Na_2Cr(Cbz)_4(THF)_3]$ (3). 36.6 mg of carbazole (HCbz, 0.22 mmol) and 0.15 mL of toluene were added to 22.7 mg of the Cr(0) nanoparticles (0.44 mmol) in an argon-filled Schlenk tube (20 mL). This Schlenk tube was heated to 80 °C for 7 days. After cooling to room temperature, yellow-brown crystals of **4** were obtained with a yield of about 50%. Here, the yield seems to be limited due to the amount of THF adsorbed on the Cr(0) nanoparticles.

$[Cr(MPy)_3]\cdot 0.5$ Tol (4). 97.2 mg of 2-mercaptopyridine (HMPy, 0.88 mmol) and 0.2 mL of toluene were added to 22.7 mg of the Cr(0) nanoparticles (0.44 mmol) in an argon-filled Schlenk tube (20 mL). This Schlenk tube was heated to 50 °C for 7 days. After cooling to room temperature, deep-green crystals of **3** were obtained with a yield of about 90%.

$[Cr_2(Bz)_4(THF)_2]$ (5). 80.1 mg of benzoic acid (HBz, 0.66 mmol) and 0.2 mL of toluene were added to 22.7 mg of the Cr(0) nanoparticles (0.44 mmol) in an argon-filled Schlenk tube (20 mL). This Schlenk tube was heated to 80 °C for 7 days. After cooling to room temperature, red crystals of **5** were obtained with a yield of about 80%.

Analytical techniques. Further details related to the analytical equipment and single-crystal structure analysis are summarized in the Supporting Information. Further details of the crystal structure investigations may be obtained from the joint CCDC/FIZ Karlsruhe deposition service on quoting the depository numbers 2269548–2269552.

Acknowledgements

A.R. and C.F. acknowledge financial support from the Deutsche Forschungsgemeinschaft (DFG, German Research Foundation) through the Collaborative Research Centre *"4f for Future"* (CRC 1573, project number 471424360), project A4. Furthermore, we acknowledge the Karlsruhe Nano Micro Facility (KNMF) at the KIT as well as Prof. Dr. Dieter Fenske and Dr. Andreas Eichhöfer for data collection on a Stoe StadiVari diffractometer with Ga-metal-jet source (compound **1** + **2**). Furthermore, the authors thank Prof. Dr. Peter Roesky, Dr. Michael Gamer and Dr. Adrian Hauser for data collection on a Stoe Stadi Vari diffractometer (compound **5**). Open Access funding enabled and organized by Projekt DEAL.

Conflict of Interest

The authors declare no conflict of interest.

Data Availability Statement

The data that support the findings of this study are available from the corresponding author upon reasonable request.

Keywords: Chromium nanoparticles · reactivity · follow-up reaction · crystal structure

[1] N. Wiberg, E. Wiberg, A. F. Holleman, *Anorganische Chemie*, de Gruyter, Berlin **2017**, 103. Ed., Vol. 1, Annex III/IV.
[2] R. P. Frankenthal, *J. Electrochem. Soc.* **1967**, *114*, 542–547.
[3] P. Schmuki, *J. Solid State Electrochem.* **2002**, *6*, 145–164.
[4] C. Feldmann, *Angew. Chem. Int. Ed.* **2013**, *52*, 7610–7611.
[5] R. D. Rieke, K. Gfele, E. O. Fischer, *J. Organomet. Chem.* **1974**, *76*, 19–21.
[6] a) M. Bedolla-Hernández, G. Rosano-Ortega, F. J. Sánchez-Ruiz, J. Bedolla-Hernández, P. S. Schabes-Retchkiman, C. A. Vega-Lebrún, *Chem. Eng. Sci.* **2022**, *252*, 117291; b) R. D. Tilley, D. A. Jefferson, *J. Mater. Chem.* **2002**, *12*, 3809–3813; c) S. Yang, C. Feng, D. Spence, A. M. A. A. Al Hindawi, E. Latimer, A. M. Ellis, C. Binns, D. Peddis, S. S. Dhesi, L. Zhang, Y. Zhang, K. N. Trohidou, M. Vasilakaki, N. Ntallis, I. MacLaren, F. M. F. de Groot, *Adv. Mater.* **2017**, *29*, 1604277.

[7] a) J. Chaudhary, G. Tailor, D. Kumar, *Mater. Today* **2020**, *29*, 321–326; b) M. Zheng, W. Li, M. Xu, N. Xu, P. Chen, M. Han, B. Xie, *Nanoscale* **2014**, *6*, 3930–3933.
[8] S. U. Son, Y. Jang, K. Y. Yoon, C. An, Y. Hwang, J.-G. Park, H.-J. Noh, J.-Y. Kim, J.-H. Park, T. Hyeon, *Chem. Commun.* **2005**, 86–88.
[9] a) C. Janiak, *Z. Naturforsch.* **2013**, *68b*, 1059–1089; b) E. Redel, R. Thomann, C. Janiak, *Chem. Commun.* **2008**, 1789–1791.
[10] a) T. Satgurunathan, P. S. Bhavan, R. D. S. Joy, *Biol. Trace Elem. Res.* **2019**, *187*, 543–552; b) O. M. Kotb, F. M. A. El-Latif, A. R. Atawia, S. S. Saleh, S. F. El-Gioushy, *Asian J. Biotechnol. Biores. Technol.* **2020**, *6*, AJB2T.57315.
[11] a) D. Bartenbach, O. Wenzel, R. Popescu, L.-P. Faden, A. Reiß, M. Kaiser, A. Zimina, J.-D. Grunwaldt, D. Gerthsen, C. Feldmann, *Angew. Chem. Int. Ed.* **2021**, *60*, 17373–17377; b) C. Schöttle, P. Bockstaller, R. Popescu, D. Gerthsen, C. Feldmann, *Angew. Chem. Int. Ed.* **2015**, *54*, 9866–9870.
[12] M. E. Straumanis, C. C. Weng, *Am. Mineral.* **1956**, *41*, 437–448.
[13] D. Zopes, B. Stein, S. Mathur, C. Graf, *Langmuir* **2013**, *29*, 11217–11226.
[14] A. M. Zieschang, J. D. Bocarsly, M. Dürrschnabel, H. J. Kleebe, R. Seshadri, B. Albert, *Chem. Mater.* **2018**, *30*, 1610–1616.
[15] R. Essmann, G. Kreiner, A. Niemann, D. Rechenbach, A. Schmieding, T. Sichla, U. Zachwieja, H. Jacobs, *Z. Anorg. Allg. Chem.* **1996**, *622*, 1161–1166.
[16] H. Lueken, *Magnetochemie*, Teubner, Stuttgart **1999**.
[17] a) F. L. Benedito, T. Petrenko, E. Bill, T. Weyhermueller, K. Wieghardt, *Inorg. Chem.* **2009**, *48*, 10913–10925; b) A. R. Hermes, R. J. Morris, G. S. Girolami, *Organometallics* **1988**, *7*, 2372–2379; c) D. C. Bradley, M. B. Hursthouse, C. W. Newing, A. J. Welch, *J. Chem. Soc. Chem. Commun.* **1972**, *9*, 567–568.
[18] a) A. E. Ashley, A. R. Cowley, J. C. Green, D. R. Johnston, D. J. Watkin, D. L. Kays, *Eur. J. Inorg. Chem.* **2009**, *17*, 2547–2552 ; b) J. C. Ott, D. Isak, J. J. Melder, H. Wadepohl, L. H. Gade, *Inorg. Chem.* **2020**, *59*, 14526–14535.
[19] A. Sousa-Pedrares, M. L. Durán-Carril, J. Romero, J. A. García-Vázquez, A. Sousa, *Polyhedron* **2013**, *62*, 278–285.
[20] a) D. V. Baxter, R. H. Cayton, M. H. Chisholm, J. C. Huffman, E. F. Putilina, S. L. Tagg, J. L. Wesemann, J. W. Zwanziger, F. D. Darrington, *J. Am. Chem. Soc.* **1994**, *116*, 4551–4566; b) P.-J. Huang, Y. Natori, Y. Kitagawa, Y. Sekine, W. Kosaka, H. Miyasaka, *Dalton Trans.* **2019**, *48*, 908–914.
[21] A. A. Pasynskii, I. L. Eremenko, T. C. Idrisov, V. T. Kalinnikov, *Koord. Khim.* **1977**, *3*, 1205–1209.

Manuscript received: June 23, 2023
Revised manuscript received: August 11, 2023
Accepted manuscript online: August 23, 2023

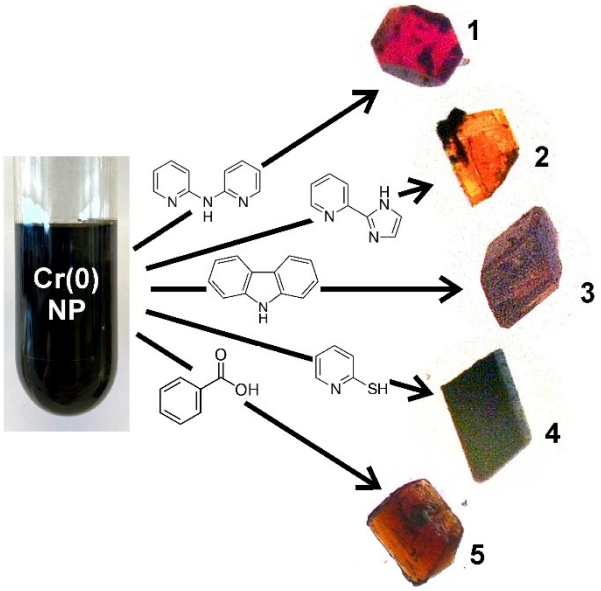

*A. Reiß, Dr. M. K. Reimann, Dr. R. Popescu, Prof. Dr. D. Gerthsen, Prof. Dr. R. Pöttgen, Prof. Dr. C. Feldmann**

1 – 10

Chromium Metal Nanoparticles, Their Reactivity and Reactions